buildings

MDPI

Article

An Exhaustive Search Energy Optimization Method for Residential Building Envelope in Different Climatic Zones of Kazakhstan

Mirzhan Kaderzhanov, Shazim Ali Memon *, Assemgul Saurbayeva and Jong R. Kim

Department of Civil and Environmental Engineering, School of Engineering and Digital Sciences, Nazarbayev University, Nur-Sultan 010000, Kazakhstan; mirzhan.kaderzhanov@alumni.nu.edu.kz (M.K.); assemgul.saurbayeva@nu.edu.kz (A.S.); jong.kim@nu.edu.kz (J.R.K.)

* Correspondence: shazim.memon@nu.edu.kz; Tel.: +7-778-443-85-16

Abstract: Nowadays, the residential sector of Kazakhstan accounts for about 30% of the total energy consumption. Therefore, it is essential to analyze the energy estimation model for residential buildings in Kazakhstan so as to reduce energy consumption. This research is aimed to develop the Overall Thermal Transfer Value (OTTV) based Building Energy Simulation Model (BESM) for the reduction of energy consumption through the envelope of residential buildings in seven cities of Kazakhstan. A brute force optimization method was adopted to obtain the optimal envelope configuration varying window-to-wall ratio (WWR), the angle of a pitched roof, the depth of the overhang shading system, the thermal conductivity, and the thicknesses of wall composition materials. In addition, orientation-related analyses of the optimized cases were conducted. Finally, the economic evaluation of the base and optimized cases were presented. The results showed that an average energy reduction for heating was 6156.8 kWh, while for cooling it was almost 1912.17 kWh. The heating and cooling energy savings were 16.59% and 16.69%, respectively. The frontage of the building model directed towards the south in the cold season and north in the hot season demonstrated around 21% and 32% of energy reduction, respectively. The energy cost savings varied between 9657 to 119,221 ₸ for heating, 9622 to 36,088 ₸ for cooling.

Keywords: building envelope; optimization; OTTV; energy consumption; Brute Force Algorithm

check for updates

Citation: Kaderzhanov, M.; Memon, S.A.; Saurbayeva, A.; Kim, J.R. An Exhaustive Search Energy Optimization Method for Residential Building Envelope in Different Climatic Zones of Kazakhstan. *Buildings* **2021**, *11*, 633. https://doi.org/10.3390/buildings11120633

Academic Editor: Roberto Alonso González Lezcano

Received: 29 October 2021
Accepted: 28 November 2021
Published: 10 December 2021

Publisher's Note: MDPI stays neutral with regard to jurisdictional claims in published maps and institutional affiliations.

Copyright: © 2021 by the authors. Licensee MDPI, Basel, Switzerland. This article is an open access article distributed under the terms and conditions of the Creative Commons Attribution (CC BY) license (https://creativecommons.org/licenses/by/4.0/).

1. Introduction

In Kazakhstan, the high demand for residential energy consumption is considered an important factor influencing economic development and domestic comfort. Energy-based economic relationships and domestic use constitute about 80% of the total energy distribution in Kazakhstan [1]. The electricity and heat generation is obtained from at least 40% of the total direct energy supply (TDES) and they are counted as one-third of the total final energy (TFEC) consumption. The ratio of TFEC to TDES, as an indicator of energy balance, shows the value as less than 50% for Kazakhstan and 69% for entire the world [2].

Kazakhstan's existing residential building stock comprises around 347.4 million square meters, almost the one third of which are outdated inefficient buildings that were constructed during the Soviet era [3]. In the 1960s, large-panel residential building projects for seismically active locations were planned and realized, while in the 1970s, the high-rise building development (from 9 to 12 stories) began. During this time, standard projects were developed that established a qualitatively new approach to standard design and expanded throughout Kazakhstan's cities [4]. The majority of the current housing stock is made up of multifamily structures that are connected to district heating via boiler houses or cogeneration stations, the rest is accounted for in unfamiliar and semi-detached houses [5,6].

Energy standards or regulations for buildings are considered an important factor in energy efficiency strategies. These codes contain details about building energy conservation methods, propose and evaluate the development of different types of energy-efficient building designs, create a specific regulation to assess building energy conditions, and propose new energy efficiency procedures for climate regions or countries [7]. Typical energy efficiency indices are perimeter annual load (PLA), envelope energy load (ENVLOAD), and overall thermal transfer value (OTTV) [6]. The PLA is the total yearly cooling and heating load in the perimeter of buildings per unit floor area; it comprises heat conduction through the envelope produced by temperature differences between outside and inside conditions, indoor heat gain, fresh air load, and solar radiation heat gain [8]. ENVLOAD is a multilinear regression equation and is commonly used for office buildings, with a focus on the thermal and optical properties of windows [9]. It is used to calculate the annual cooling load of the perimeter area and represents maximum allowable loads through the building envelope. The internal heat gains and efficiency requirements of the HVAC system contribute to controlling the cooling energy areas [10]. In the ENVLOAD method, the impact of indoor thermal comfort is not consolidated and the analysis of the energy performance of the building cannot be investigated for further changes and corrections. In addition, it is mostly applied to cooling predominant regions [11–14]. The overall thermal transfer value is a measurement of the average heat gain moving into a building through the building envelope that may be used to compare thermal performance between different building designs [15]. The OTTV is a measurement of the average heat gain moving into a building through the building envelope that may be used to compare the thermal performance between different building designs [15]. The main advantage of this method is the simplicity of calculation in terms of flexibility on the relationship between compositions of the building envelope. On the other hand, the negative aspects are that it does not consider the interaction between envelope, internal gains, and chiller efficiency [9]. However, OTTV can safely be used for evaluating the heating energy performance of the building model based on solar energy entering during the construction stage.

Zero-energy concept, low carbon future, and reduction of resources that affect construction, demolition, operation, and disposal of land-based factors are an important concept in residential buildings [7]. From an environmental point of view, energy efficiency has been mentioned as one of the most influential issues in building design. Discrete optimization methods and technological innovations can minimize the energy consumption of any energy-related system. One of such methods is called the brute force algorithm. Local search by brute-force (BF), also known as the exhaustive search method, is a global algorithmic approach for dealing with computationally multi-objective optimization problems [16]. The brute force approach has the advantage of searching all possible outcomes in the system [17], but can be computationally time-consuming when working with large and complex datasets. Despite this disadvantage, the BF approach is relevant for spatial analysis in the era of the massive data source in the context of demographic analysis or public health analysis [17]. This is exhaustive, as it becomes widespread when possibly scaling computer force to solve a problem on demand. It has been widely used for optimizing building envelope systems, as indicated in the literature [18].

Basically, construction standards determining the requirements regarding the energy efficiency of residential buildings are not commonly observed to construct a new building to decrease construction estimate costs. In addition, there are no mandatory energy standards in Kazakhstan regarding the maintenance and operation of the housing energy-related works, including those concerning the level of energy efficiency [6]. Thus, it was decided to use OTTV for the energy performance of the building model for the construction stage only by using the weather data of different cities in Kazakhstan. In this research, an OTTV-based building energy simulation model (BESM) integrated by using a brute-force optimizer was developed to significantly cut the energy consumption of residential buildings located in different cities of Kazakhstan. For this purpose, the heating and cooling energy demands were reduced by deeply investigating the performance of the following building envelope components: window-to-wall ratio, thermal and dimensional parameters of the wall, angle of the pitched roof, and depth of the overhang shading system. The validity of BESM was demonstrated by performing an energy analysis of a real townhouse building located in seven different cities of Kazakhstan (Nur-Sultan, Almaty, Karaganda, Aktobe, Atyrau, Kokshetau, and Semey). Finally, the comparative cost analysis of the base and the optimized cases obtained from the BESM was presented.

2. Methodology

This research focuses on the development of the OTTV-based building energy simulation model (BESM) for the reduction of the energy consumption through the envelope and by obtaining the optimal envelope configuration for residential buildings of Kazakhstan. This section presents the base and derived OTTV-based heat transfer analysis equations for heating and cooling; the characteristics of the building envelope; proposed equations, simulation, and optimization models; and case study. For the implementation of this approach, the modified mathematical model of OTTV was formulated, and the building energy simulation model was developed. After simulation, the brute force algorithm was applied to obtain the optimum solutions for heating and cooling energies. The reliability of the numerical model was verified against the simulation model, which was calibrated by comparison of the single-room building performance for heating energy consumption. Finally, the case study parameters, including building model and climate condition in selected cities, are presented. Figure 1 shows the framework of the proposed BESM and optimization method.

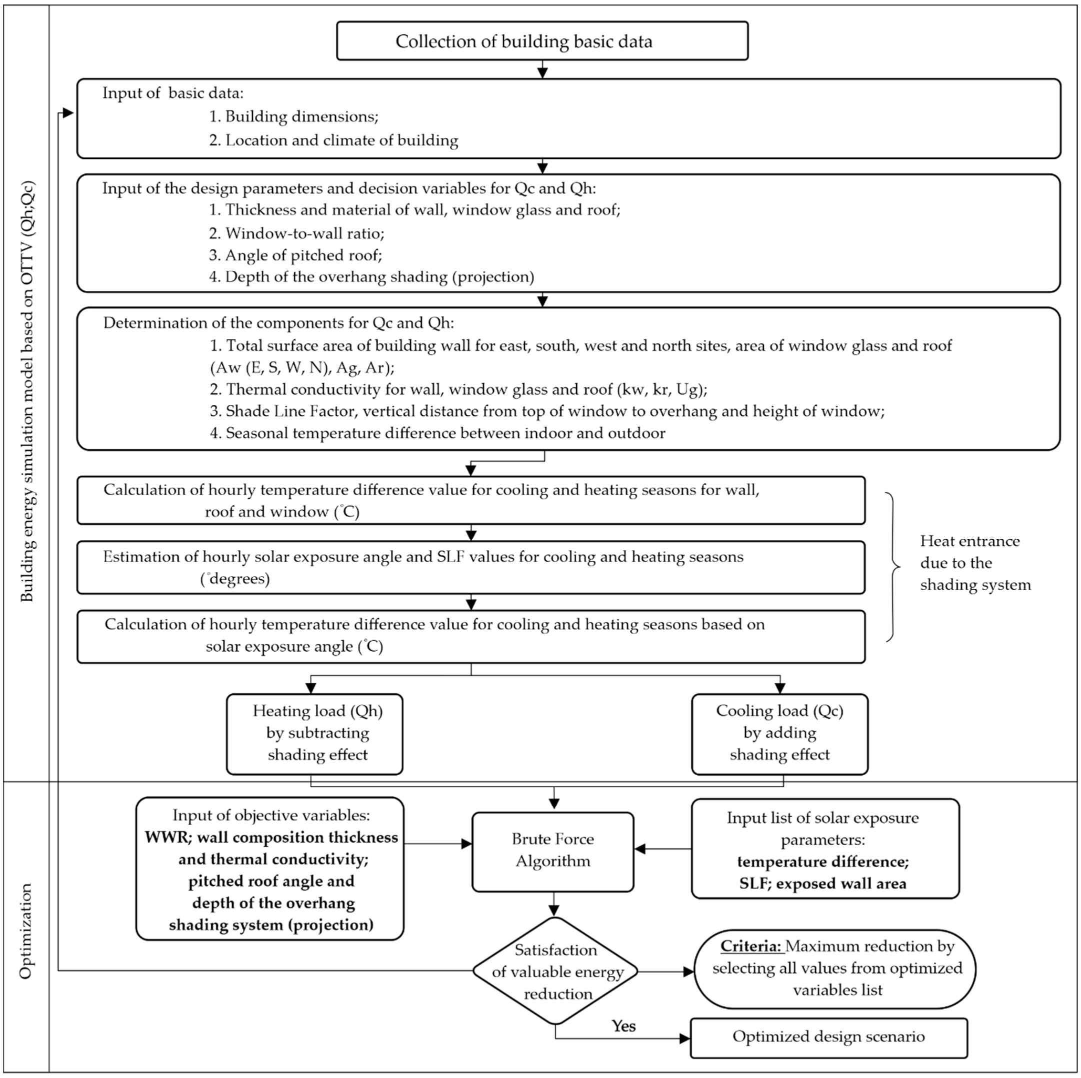

Figure 1. Flowchart of the BESM and optimization. Note: Q_c is a heat gain through the envelope for the cooling season; Q_h is a heat loss through the envelope for the heating season; A_w, A_g, and A_r are the surface area of the wall, window, and roof; k_w is the overall thermal conductivity of the wall; k_r is the thermal conductivity value of the roof; and U_g is the U-value of glazing.

2.1. The Overall Thermal Transfer Value (OTTV)

The OTTV standard is the maximum allowable heat gain value in cooling-dominant regions, calculated for a building or part of a building in W/m^2 [10]. Typically, two sets of OTTV are used, one for the external walls and the other for the roof [19]. For an exterior wall, the typical form of the OTTV equation isas follows:

$$OTTV_{wall} = \frac{Q_{wc} + Q_{gc} + Q_{gsol}}{A_{wall}} \quad (1)$$

where A_{wall} is the exterior wall's gross area, Q_{wc} is the conduction through the opaque wall, Q_{gc} is the conduction through the fenestration, and Q_{gsol} is the solar radiation through the fenestration. Heat transfer through an opaque wall is induced by a temperature difference between outside and indoor regions, as well as a solar radiation incident on the opaque wall Q_{wc} [19].

If the computed number from Equation (1) is equal to or less than an OTTV limit specified in an OTTV regulation, the OTTV requirement is deemed as being met. The basic assumption is that the higher the OTTV value, the greater the net heat gain through the building envelope and, as a result, the more energy required for cooling [20]. OTTV can provide building designers more flexibility for inventive design by considering the different components of building heat gain and allowing for trade-offs between them. In the energy-efficient building envelope design, OTTV is acknowledged as a simple and effective regulation [21]. The OTTV is used to measure average heat gain passing into the indoor area through the building envelope. Therefore, it can serve as an index of the impact of the envelope on the cooling energy utilized in air-conditioned buildings [20]. By changing the indoor setpoint temperature and reverse effect of the shading system compared with the cooling case, the heat loss equation was also developed for application during the heating season [21]. It consists of two measures, namely: envelope thermal transfer value (ETTV) and roof thermal transfer value (RTTV). The following equations demonstrate the calculation of ETTV and RTTV, respectively [22]:

$$ETTV = \frac{\sum Q}{\sum A} = \frac{Q_{wc} + Q_{gs}}{A_w + A_g} \quad (2)$$

$$Q_{wc} = A_w \times U_w \times \alpha_w \times TD_{eqw} \quad (3)$$

$$Q_{gs} = A_g \times SC \times ESM \times SF \quad (4)$$

$$RTTV = \frac{A_r \times U_r \times \alpha_r \times TD_{eqr}}{A_r} \quad (5)$$

where A_w, A_g, and A_r are the area of the wall, window, and roof, respectiy; Q is the a heat transfer through the envelope; U is the thermal transmittance of a specific material, α is the solar absorptivity constant related to the façade surface and color; TD is the equivalent temperature difference; SC is the shading coefficient of the glazing; ESM is the external shading multiplier; and SF is the solar factor (W/m^2).

As indicated in Equations (2)–(5), the areas (A_w, A_g, and A_r) and physical characteristics (U_w, U_r, α_w, α_r, and SC) of the building envelope, as well as the climate-dependent factors (TD_{eqw}, TD_{eqr}, and SF), are the key variables for determining the OTTV of a building [15]. OTTV enables the building designer to make trade-offs between various envelope characteristics such as U (value for the wall and roof (U_w and U_r, respectively)), shading coefficient (SC), etc.

2.2. Building Envelope Parameters

The building envelope is the component of the structure that physically divides the indoor and the outdoor environments [23]. It is reported that the majority of indoor cooling and heating loads are generated by heat gain and heat loss via building external envelopes such as walls, windows, and ceilings, which are caused by the difference in indoor and outdoor temperatures [24]. The temperature difference between indoor and outdoor conditions essentially affects the total energy consumption of the residential building in cold and moderate climate regions. The heating energy dominates rather than the cooling energy in the continental climate zone, such as Kazakhstan. Thus, for significant energy savings, while maintaining occupant thermal comfort, careful consideration of heat transfer through the envelope is critical [23]. The optimization of heat transfer based on envelope composition is investigated to reduce the building energy consumption. The details of the building model parameters including external sunshade, wall composition materials, and roof composition materials are provided and discussed in the next sections.

The heat gain and heat loss equations based on the OTTV method were developed by considering the boundary properties, such as indoor setpoint temperature, hourly outdoor dry-bulb temperature, hourly solar exposure, envelope material characteristics, and climate conditions [25].

Design Variables

In this research, the main variables used for OTTV determination are divided into two categories: endogenous and exogenous. Endogenous variables describe the particular effect on the model that is dependent on a variety of factors on the model [26]. These variables are the wall area, window glazing area, roof area, roof ceiling area, thermal resistance of ceiling, thermal resistance of the roof, vertical offset from shading to top of the window, height of the window, U-value of glazing, standard solar heat gain coefficient of glazing (SHGC), thermal conductivity, and window-to-wall ratio (WWR). Exogenous variables, in turn, are variables whose origin is outside of the model and whose purpose is to explain other variables or outcomes [27]. The temperature difference between the indoor set point and outdoor dry-bulb temperature, area of the wall exposed by solar radiation at specific times, shade line factor values based on the angle of solar radiation, heating and cooling loads, thickness of wall materials, angle of pitched roof, and depth of overhang shading (projection) are considered as exogenous variables in this research. The detailed chart regarding the connection between endogenous and exogenous variables and their consistency is shown in Figure 2.

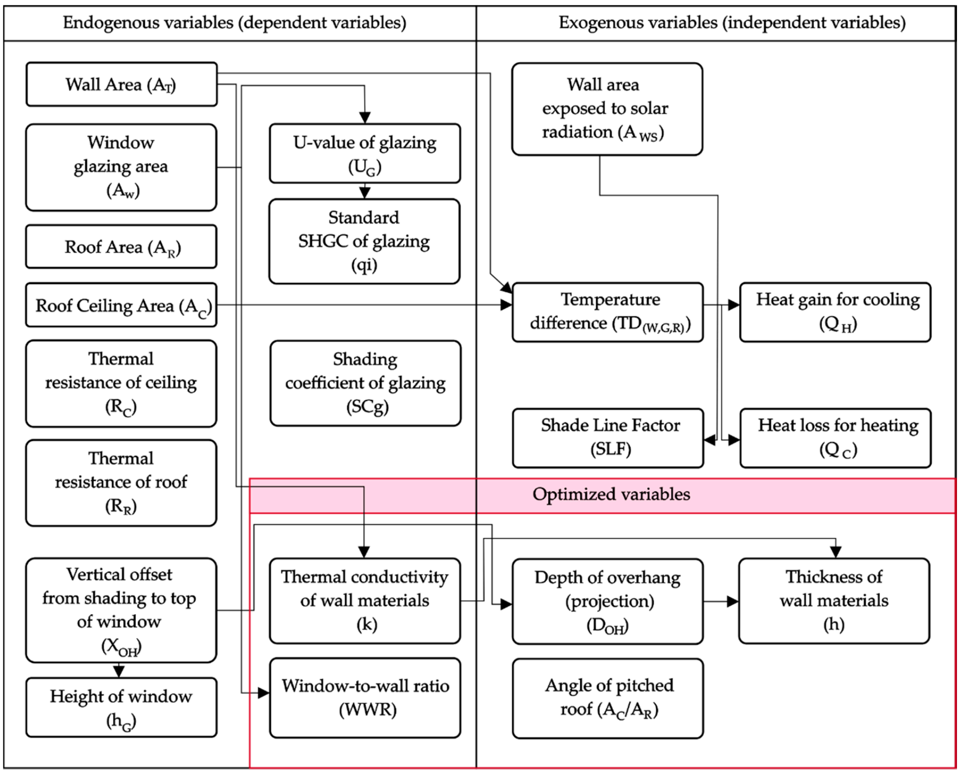

Figure 2. Components of the building energy simulation model and connection between the endogenous and exogenous variables.

2.3. Formulation of a Model

To provide the overall formulation of the analysis, the following assumptions were made in the model. (1) The wall materials were considered to be thermally isotropic and homogeneous. (2) The heat transfer mechanism was assumed to be two-dimensional, where the direction of the building's height was disregarded [28]. (3) The thermal conductivity value for all composition materials was constant. (4) Any sub-cooling or sub-heating activities were not included.

The heat gain and heat loss through the envelope were composed of four components: heat transfers through the walls, roof, and windows produced by differences in internal and external temperatures, and solar radiation heat transfer through the windows in terms of a shading system [19]. The following detailed mathematical models were developed from Equations (2)–(5) and present heat transfer through unit area of building envelope based on the temperature difference between indoor and outdoor for cooling and heating seasons:

$$Q_c = \sum_{i=1}^{n} k_{w_i} \times A_{w_i} \times \Delta TD_{w_c} + k_r \times A_r \times \Delta TD_{rc} + \sum_{i=1}^{m} U_g \times A_{g_i} \times \Delta TD_{gc} + \sum_{i=1}^{m} q_{ic} \times SC_{ic} \times A_{wsi} \times \Delta TD_{gc} \quad (6)$$

$$Q_h = \sum_{i=1}^{n} k_{w_i} \times A_{w_i} \times \Delta TD_{w_h} + k_r \times A_r \times \Delta TD_{rh} + \sum_{i=1}^{m} U_g \times A_{g_i} \times \Delta T_h - \sum_{i=1}^{m} q_{ih} \times SC_{ih} \times A_{wsi} \times \Delta TD_{gc} \quad (7)$$

where Q_c is a heat gain through the envelope for the cooling season; Q_h is a heat loss through the envelope for the heating season; k_w is an overall thermal conductivity of the wall; TD_w, TD_r, and TD_g are equivalent temperature differences between indoor and outdoor surrounding space wall, roof, and glazing, reseptively; q is the standard solar heat gain factor; U_g is the U-value of glazing; A_w, A_g, and A_r are the surface area of the wall, window, and roof; A_{wsi} is wall area exposed to solar radiation; SC is the total shading coefficient; n and m are the numbers of external walls and windows; subscripts w, r, and g are external wall, roof, and external window, respectively; subscript i shows the various orientations; subscripts c and h represent the cooling and heating periods, respectively.

The overall thermal conductivity of the wall can be calculated as follows:

$$k_w = \frac{1}{\frac{h_1}{C_1} + \frac{h_2}{C_2} + \frac{h_3}{C_3} + \frac{h_4}{C_4}} \quad (8)$$

where h_1, h_2, h_3, and h_4 are the thicknesses of the wall composition layers, and C_1, C_2, C_3, and C_4 are the thermal conductivity values of wall composition layers.

$$A_T = A_{T_E} + A_{T_S} + A_{T_W} + A_{T_N} \quad (9)$$

The overall thermal conductivity of the roof can be calculated as follows:

$$k_r = \frac{1}{R_c + R_r \times \frac{A_c}{A_r}} \quad (10)$$

where k_r is the thermal conductivity values of the roof, R_c is the thermal resistance value for the roof ceiling, R_r is the thermal resistance value for the roof, A_c is the ceiling area, A_r is the roof area, and $A_T(E, S, W, N)$ is the total area building's wall.

$$A_w = (1 - WWR) \times A_T \quad (11)$$

$$A_g = WWR \times A_T \quad (12)$$

$$SC = SC_g \times \min\left(1, \max\left(0, \frac{SLF \times D_{oh} - X_{oh}}{h_g}\right)\right) \quad (13)$$

where SLF is the shade line factor, D_{oh} is the depth of overhang (projection), X_{oh} is the vertical offset from the top of the window to the overhang, h_g is the height of the window, WWR is the window-to-wall ratio, and SC_g is the shading coefficient of the glazing.

The constant dimensional values of the building envelope, such as the wall area for each building sector, roof area, wall material thickness, and thermal transmittance through the window were set to the model. Consequently, the building's total area (A_T) for the east, south, west, and north walls were 81.2, 62.4, 93.6, and 74.4 m^2, respectively, while the roof area was calculated as 154.2 m^2. The initial WWR was kept as 5% and the U-value of the window glass was 1.978 W/m^{2}K. The area of windows was calculated by the multiplication of the total area and WWR. The solar heat gain coefficient (SHGC) is a ratio of solar radiation absorbed or transmitted through the window or door, to the heat that is released back (SHGC = 0.68). The total shading coefficient was calculated by multiplying the shading coefficient of the glazing and overhang shading system. The shading coefficient of the glazing (SC_g) was calculated by dividing the solar heat gain coefficient (SHGC) of the window by 0.86 to get 0.7988, while the standard solar heat gain factor (q) was a heat gain through 3 mm normal glass and was calculated as the ratio of the U-value and shading coefficient of the window to obtain 2.5 W/m^{2}K. The sum of the hourly temperature difference for heating and cooling was calculated using the outside dry-bulb temperature and inside set-point temperatures that were obtained from DesignBuilder software by using the weather data purchased from the White Box Technologies, Inc, Moraga, CA, USA [29]. The weather data represent the typical year, the composition of which reflects the long-term average conditions for a location over a period of 12 up to 22 years. The heating season lasted from the middle of October to the middle of May, while the cooling season lasted from the middle of May to the middle of October. The following variables of the building envelope, such as WWR, wall composition layer thicknesses, thermal conductivity of wall composition materials, depth of the overhang normal to the building plane, and ratio of ceiling area to the roof area (angle of the pitched roof) were optimized by the proposed energy estimation model.

2.3.1. Heat Transfer through the Pitched Roof

The roof structure of the modeled building was assumed to be pitched with the unvented attic. Unvented attics are effective for the reduction of energy loss through ceiling facilities or leaky channels. The average value for energy savings by unvented attics was counted as 20% [30]. For the roof with the unvented attic, the heat transfer procedure occurred through three different mediums, namely the ceiling, roof, and attic itself. Thus, the overall thermal resistance value of the roofing system was directly related to the individual thermal resistance values of the roof and ceiling combined with the thermal resistance of the attic space. Attic space may be assumed as an air layer in the composition. In most cases, the practical influence of attic space accounted for the surface thermal resistance of the roof and ceiling adjacent to the space. The thermal resistance values for the roof and ceiling were determined separately using convection resistance case for still-air in the attic surface [31]. Thus, the overall R-value for the combination of ceiling−roof is expressed as follows:

$$R = R_{ceiling} + R_{roof} \times \frac{A_{ceiling}}{A_{roof}} \tag{14}$$

$$k_r = \frac{1}{R_{ceiling} + R_{roof} \times \frac{A_{ceiling}}{A_{roof}}} \tag{15}$$

where $A_{ceiling}$ and A_{roof} are the ceiling and roof areas, respectively, while $R_{ceiling}$ and R_{roof} are thermal resistance values for ceiling and roof and equal to 0.1328 m^2 K/W and 0.8733 m^2 K/W, respectively. If the area ratio is equal to one, the roof is flat, and it is less than one for pitched roofs. For the modeled building, the initial value of angle for the roof was 27°, and the thermal conductivity (k_r) of the entire roofing system was equal to 1.1247 W/mK. Additionally, the direction of heat flow was upward (heat loss) in the cold season and downward (heat gain) in the hot season. An adequate R-value for unvented roofing required the usage of appropriate materials with proper workmanship that met the standards. Otherwise, the usage of inappropriate materials and poor workmanship could lead to the R-value being different from the predicted one. The thermal resistance structure for a pitched roof—attic—ceiling case with an unvented attic is presented in literature [31].

2.3.2. Details of Overhang Shading Device Configuration

The location of the shading material plays an important role in the solar gain control process. The outdoor shading system can contribute to a substantial reduction in heat gains, but requires adequate regular maintenance and is difficult to install. On the contrary, an indoor shading system cannot be as effective as controlling solar heat gain quantity, but it is easier to install. Shading systems depend on glazing type, material, and shading properties [32,33]. The U-value of the fenestration system cannot be changed by the application of the shading system [34]. However, most of the shading systems can afford to insulate the heat and are used as an additional improvement for the thermal conductivity of the window, especially if they are tightly installed at a specific position with no air infiltration. Shading devices are intended to control daylighting and thermal control challenges of the building [35]. For fenestration systems of the modeled building, the simple overhang-shading device (Figure 3) was installed. The vertical offset from the top of the window to the shading device (X_{oh}) was kept as 0.2 m, while the depth of the overhang normal to the building plane (projection, D_{oh}) was 0.5 m and the fenestration height was 1.5 m. The shade line factor (*SLF*) based on the angle of solar exposure was calculated on an hourly basis for the entire season, by creating Table 1, representing the month, time, and subsequent solar exposure angle.

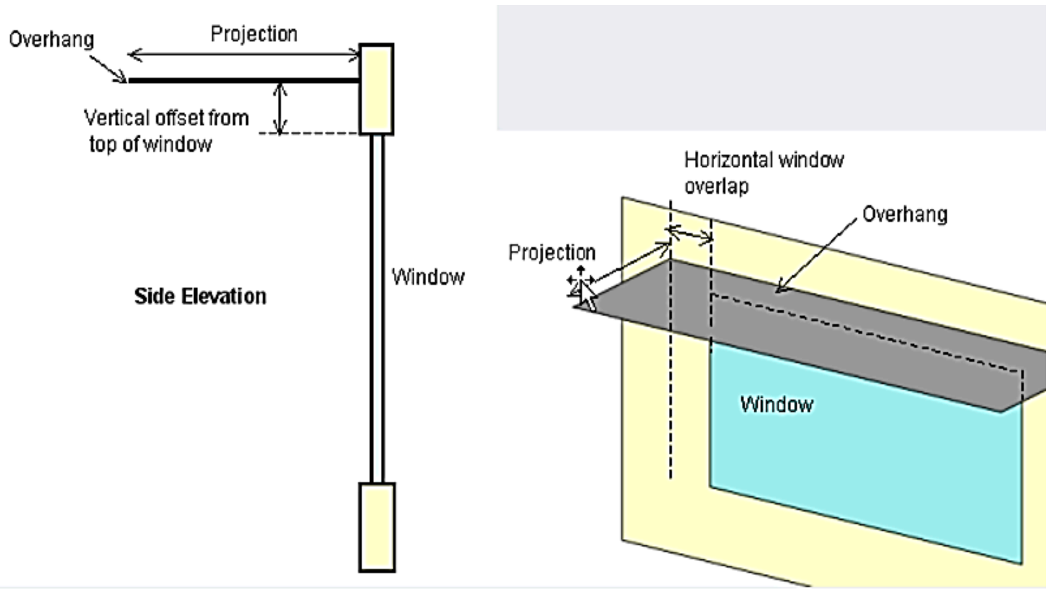

Figure 3. Details of the overhang shading device [36]. Reproduced with permission from DesignBuilder Software Ltd., (Gloucestershire, UK).

Table 1. The data collection example for the *SLF* estimation.

1st of January (Time)	Exposure Site	Angle of Sunlight (°)
9:00	southeast	4.73
10:00	southeast	10.82
11:00	southeast	15.15
12:00	southeast	17.45
13:00	southwest	17.39
14:00	southwest	14.99
15:00	southwest	10.4
16:00	southwest	3.08

The *SLF* is the ratio of the vertical distance of the shadow fall underneath the edge of the overhang to the depth of the overhang, although the shade line can be equal to the *SLF* times the depth of the overhang. Based on the angle of sunlight values evaluated in Table 1 and the shape line factors values of ASHRAE [37], the interpolation rule was used to calculate the *SLF* values for each time, month, and angle of solar exposure and to demonstrate the constant value for *SLF* at the hour with the highest solar intensity on exposures [25].

$$SCs = \min\left((1, \max\left(0, \frac{SLF \times D_{oh} - X_{oh}}{h_g}\right)\right) \quad (16)$$

where,

SC—total shading coefficient,
SLF—shade line factor from [37],
D_{oh}—depth of overhang (projection), m
X_{oh}—vertical offset from the top of the window to overhang, m
h_g—height of the window, m.

2.4. Building Design Optimization

2.4.1. Optimization Variables

In order to reach an optimal and practical design strategy, an optimization technique is required [18]. The first step in optimization is the identification of the input variables and their ranges. In this research, the optimization was performed by changing the ranges of the exogenous and endogenous design variables. The variables involved in envelope optimization include a *WWR* (4, 5, 10, 15, 20, 25, and 30%), the angle of a pitched roof (22, 27, 30, 34, 37, 40, 42, and 45°), the depth of the overhang shading system (0.5, 0.6, and 0.7 m), and the thermal conductivity and thicknesses of wall composition materials. The variable value ranges for *WWR*, the angle of a pitched roof and the depth of the overhang shading system were taken from the literature [38–40].

In this research, the wall composition consisted of four layers: exterior finish, material block (core layer), insulation layer, and interior finish (Figure 4), which were optimized. The materials utilized to construct the building envelope as well as their specifications were obtained from conventional architectural design schematics that fulfilled the requirements of Kazakhstan's building codes and standards [41–45]. Table 2 describes the detailed properties of the layers for the studied wall (thickness, thermal conductivity, specific heat, and density). The exterior finish consisted of different materials including ceramic brick, cement sand render, limestone mortar, burnt ceramic clay tile, dry ceramic clay tile, and ceramic glazed tile. The core layer consisted of masonry block, burnt brick veneer, aerated concrete block, brick veneer, reinforced concrete, and clay block. For the insulation layer: penoplex, glasswool, hydro isolation, mineral wool plate, extruded polystyrene, and cellulose were used, while for the interior finish, gypsum board, cement mortar, gypsum insulating plaster, plasterboard 1, plasterboard 2, and plasterboard 3 were used.

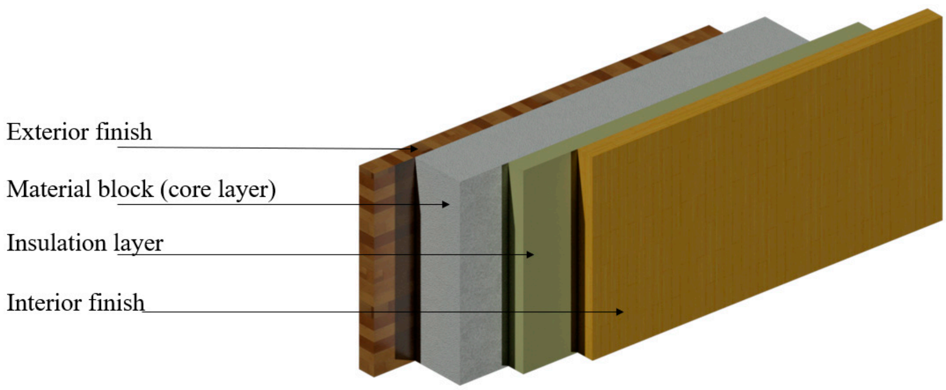

Figure 4. Cross-section view of the wall composition materials.

Table 2. Wall composition of the thermophysical properties analyzed.

Layers	Materials	Thickness, (h_1, h_2, h_3, h_4), (m)	Thermal Conductivity, (C_1, C_2, C_3, C_4), (W/mK)	Density (kg/m^3)	Specific Heat (J/kgK)
Exterior finish	Ceramic brick	0.5	0.59	1831	825
	Cement sand render	0.02	1	1800	1000
	Limestone mortar	0.02	0.7	1600	840
	Burnt ceramic clay tile	0.012	1.3	2000	840
	Dry ceramic clay tile	0.012	1.2	2000	850
	Clay block	0.0075	1.4	2500	840
Material Block (Core layer)	Masonry block	0.15	0.24	800	840
	Burnt brick veneer	0.15	0.74	1700	800
	Aerated concrete block	0.2	0.24	750	1000
	Brick veneer	0.15	0.547	1950	1000
	Reinforced concrete	0.15	0.5	1400	830
	Clay block	0.19	1.0	1800	920
Insulation layer	Penoplex	0.0795	0.030	30	1340
	Glasswool	0.012	0.039	20	840
	Hydro isolation	0.015	0.29	29	1210
	Mineral wool plate	0.1	0.036	70	810
	Extruded polystyrene	0.0795	0.03	43	1210
	Cellulose	0.2	0.04	48	1381
Interior finish	Gypsum Board	0.013	0.16	800	1090
	Cement mortar	0.012	0.72	1760	840
	Gypsum insulating plaster	0.013	0.18	600	1000
	Plaster board 1	0.012	0.72	840	1860
	Plaster board 2	0.012	0.25	600	1089
	Plaster board 3	0.012	0.35	817	1620

2.4.2. Optimization Algorithm

The second step is iteratively conducting the optimization. Before determining the optimal design solution, a brute force optimization method was utilized to analyze all design parameters. Brute force is an exhaustive search method and computational data analysis that is commonly counted as a general problem-solving method. The brute force method has an advantage in investigating all possible solutions from the list of the values but can take a long computational time with the complicated dataset [46]. Despite this, the brute force method is relevant for spatial coding analysis. As indicated in the literature [18], the method has been widely used for optimizing building envelope systems.

In order to facilitate the optimization, Python code was written to modify the design parameter. The analyzed variables in this numerical model were WWR, wall composition thicknesses, thermal conductivity of wall composition materials, and angle of the pitched roof. By investigating all of the existing possible values in the list of mentioned variables, the minimum value of heat gain (Q_c) and heat loss (Q_h) were proposed and analyzed for energy reduction compared with the value related to the initial building parameters. The detailed version of the analyzed mathematical model for the first part was computed and expressed below:

$$
\begin{aligned}
Q_1 = \left(A_{T_E} + A_{T_S} + A_{T_W} + A_{T_N}\right) \times (1 - WWR) \times \frac{1}{\frac{h_1}{C_1} + \frac{h_2}{C_2} + \frac{h_3}{C_3} + \frac{h_4}{C_4}} \times \sum_{i=1}^{n} \Delta TD_w \\
+ \frac{1}{R_c + R_r \times \frac{A_c}{A_r}} \times A_c \times \sum_{i=1}^{n} \Delta TD_r \\
+ U_g \times WWR \times \left(A_{T_E} + A_{T_S} + A_{T_W} + A_{T_N}\right) \times \sum_{i=1}^{n} \Delta TD_g
\end{aligned}
\tag{17}
$$

where TD_w, TD_r, and TD_g are the equivalent temperature differences between indoor and outdoor surrounding space wall, roof, and glazing, respectively; q is the standard solar heat gain factor; U_g is the U-value of glazing; h_1, h_2, h_3, and h_4 are the thicknesses of wall composition layers; C_1, C_2, C_3, and C_4 are the thermal conductivity values of the wall composition layers; R_c is thermal resistance value for roof ceiling; R_r is thermal resistance value for the roof; A_c is the ceiling area; A_r is roof area; $A_T(E, S, W, N)$ is the total area building's wall; and WWR is the window-to-wall ratio.

The analysis of the shading properties of the glazing is quite complicated, as the values for hourly temperature difference, the hourly orientation of solar exposure and hourly SLF values are considered in the second script. Primarily, to find the unique optimum value for WWR in both scripts, the second part of the equation is calculated without the WWR value. This partial equation is estimated by exporting the hourly values from the spreadsheet (Table 3) for the wall area of the entire building exposed by the solar radiation (A_{ws}), temperature difference, and SLF. Table 3 represents the hourly temperature difference, area of the wall exposed to sunlight, and corresponding shade line factor (SLF) value for the numerical model analysis.

Table 3. The data collection example of the hourly shading system performance.

1-st of January	Temperature Difference (°C)	Shade Line Factor	Wall Area Exposed to Solar Radiation (m^2)
9:00	37.58	2.43	144
10:00	36.98	2.29	144
11:00	36.2	2.18	144
12:00	35.4	2.13	144
13:00	34.6	2.13	156
14:00	33.88	2.19	156
15:00	33.4	2.30	156
16:00	33.53	2.47	156

The summation ofthe estimated values for each hour in each analyzed season are varied by the list of values of overhang shading depth, which means that for each value of overhang depth there are computed values of Q_2. The wall area exposed by solar radiation varies hour by hour, as the sunlight rises from the east and rests west. Each selected WWR value was multiplied by the resulting values of Q_2 to find the maximum and minimum values of Q_2 in the heating and cooling seasons, respectively. The maximum and minimum values of Q_2 were defined by the "−" and "+" signs before this expression, as an expression of Q_2 describes the reduction of heat entering into the indoor area by the shading system. The heat gain equation for cooling (Q_1) should add the minimum value of heat gain reduction value (Q_2), while the heat loss equation for heating (Q_1) should subtract the maximum value of heat gain reduction (Q_2) to get the overall value for heat transfer as minimum as possible to be optimized. The detailed version of the analyzed mathematical model for the heat gain reduction by the shading system was computed and is expressed below.

$$Q_2 = q_{ih} \times WWR \times (A_{ws}) \times SC_g \times \sum_{i=1}^{n} \Delta TD_{wi} \times \min\left(1, \max\left(0, \frac{SLF_i \times D_{oh} - X_{oh}}{h_g}\right)\right) \quad (18)$$

where q is the standard solar heat gain factor; WWR is the window-to-wall ratio; A_w is a surface area of the wall; SC_g is the shading coefficient of the glazing; TD_w is the equivalent temperature differences between indoor and outdoor surrounding space wall; SLF is shade line factor from; D_{oh} is the depth of overhang (projection); X_{oh} is vertical offset from the top of the window to overhang; and h_g is the height of the window.

Finally, the combination of the two parts appears in the following way: Q_1 for heating minus the maximum value of Q_2 for heating, and Q_1 for cooling plus the minimum value of Q_2 for cooling to obtain the minimum energy consumption in heating and cooling seasons. Based on the iterative summation of the second part due to the large data obtained from the spreadsheet, the running process of the coding takes an insignificant amount of time. The optimized results, by highlighting all optimum values of iterative variables and the final value of the entire energy equation heating and cooling, are shown in the Results and Discussion chapter.

2.5. Verification of Results between Building Energy Simulation Model and DesignBuilder Software

In this research, the reliability of the numerical model developed to calculate the energy transfer performance in Python software was validated. The heating load performance results between the simulation and numerical models were compared. For this purpose, a single-room building (Figure 5) with dimensions of 5.0 m × 5.0 m × 3.0 m, with an overhang shading system was modeled in Design Builder software. The material properties of the wall and roof are provided in Table 4. The *WWR* ratio was kept as 5% and the height of windows was 1.5 m. The overhang shading system was installed with a depth (projection) of 0.5 m. The weather data of Nur-Sultan was used for this verification. The numerical model-based analysis was also conducted for temperature conditions and sunshade performances developed for Nur-Sultan city.

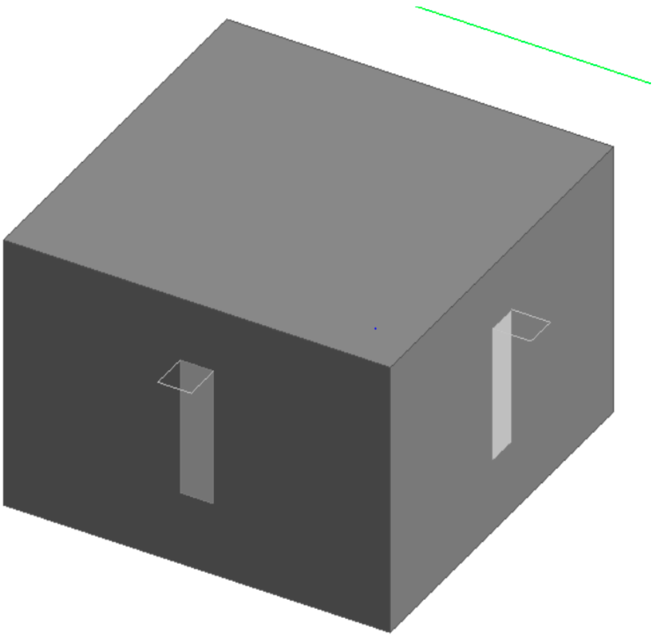

Figure 5. The model of the single-room building.

Table 4. Thermophysical properties of the building envelope materials.

Composition Materials	Layers	Material	Thickness, (h_1, h_2, h_3, h_4), (m)	Thermal Conductivity, (C_1, C_2, C_3, C_4), (W/mK)	Density (kg/m^3)	Specific Heat (J/kgK)
Wall	Exterior finish	Burnt ceramic clay tile	0.012	1.3	2000	840
	Core layer	Brick veneer	0.0165	0.542	1950	840
	Insulation	Glasswool	0.081	0.039	20	840
	Interior finish	Plaster board	0.0125	0.35	817	1620
Roof	Exterior finish	Roof tile	0.01	0.84	1900	800
	Core layer	Concrete slab	0.15	1.13	2000	1000
	Insulation	Polystyrene	0.2423	0.29	29	1210
	Interior finish	Roofing felt	0.005	0.19	960	837

The results of the numerical model and simulation are shown in Figure 6. According to the results, the maximum percentage difference between the numerical model and simulation-based results did not exceed 7.7%. Thus, it can be concluded that numerical model-based results with materials' thermal characteristics can be used and optimized for energy load performance.

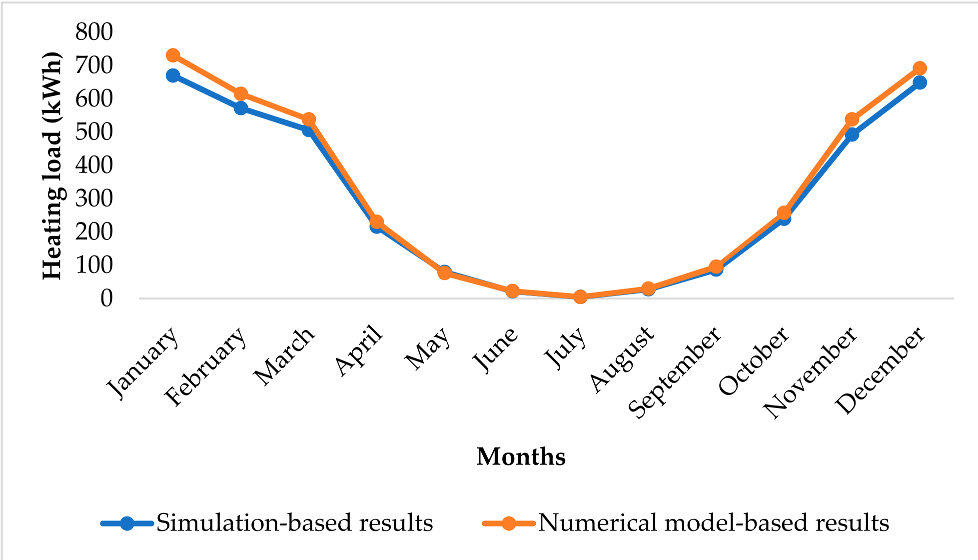

Figure 6. Simulation-based results vs. numerical model-based results.

2.6. Case Study

2.6.1. Climate Conditions

The Koppen climate classification is a widely used climate classification system that has been used since 1900. According to the background that was proposed over a century ago, the Koppen−Geiger world map was created based on monthly precipitation and temperature performance over a long period. The climates are defined by different letter symbols: A (tropical), B (arid), C (temperature), D (cold), and E (polar). Kazakhstan area has five different climate zones. There are hot-summer humid continental climate (Dfa), warm summer humid continental climate (Dfb), cold semi-arid climate (Bsk), cold desert climate (Bwk), and the Mediterranean influenced hot summer continental climate (Dsa) [45]. Based on these climate zones, seven cities were selected and shown in Figure 7. It is important to note that Kazakhstan has four seasons, namely winter (from December to February), spring (from March to May), summer (from June to August), and autumn (from September to November). January is counted as the coldest month based on the lowest average monthly temperature, while July is the hottest month. The details of the climate parameters, along with the average temperature in the hottest and coldest months are reflected in Table 5. The average temperature data were selected from the Climate Data website [47]. According to the cold season, Nur-Sultan, Karaganda, and Semey from the Dfb climate zone demonstrate average temperatures, with −18.3 °C, −14.2 °C, and −12.2 °C in the coldest month, respectively. Almaty and Aktobe are from the Dfa climate zone and have average temperatures of −8.4 °C and −16.5 °C, respectively. The average temperature in January for Atyrau from the Bwk climate zone and Kokshetau from the Bsk climate zone are −9.9 °C and −19.7 °C, respectively. During the hot season, the average temperatures of the hottest month in Nur-Sultan, Karaganda, and Semey from the Dfb climate zone are 20 °C, 18 °C, and 18 °C, respectively. Almaty and Aktobe cities from the Dfa climate zone have average temperatures in July measured as 24 °C and 27 °C, respectively. Atyrau city from the Bwk climate zone and Kokshetau city from the Bsk climate zone demonstrate the average outside temperatures in July of 27 °C and 20 °C, respectively.

Figure 7. Location of selected cities.

Table 5. Climate parameters of selected cities.

City	Latitude	Longitude	Climate Zone (According to Koppen Classification)	The Average Temperature in January (°C)	The Average Temperature in July (°C)
Nur-Sultan	51.18	71.45	Dfb	−18.3	20
Almaty	43.25	76.92	Dfa	−8.4	24
Karaganda	49.83	73.16	Dfb	−14.2	18
Aktobe	43.25	67.76	Dfa	−16.5	25
Atyrau	47.11	51.88	Bwk	−9.9	27
Semey	50.41	80.20	Dfb	−12.2	18
Kokshetau	53.28	69.39	Bsk	−19.7	20

2.6.2. Building Model

For this research, a townhouse was analyzed (Figure 8) in seven different cities (Nur-Sultan, Almaty, Karaganda, Aktobe, Atyrau, Semey, and Kokshetau) of Kazakhstan. This building was analyzed by facing the west direction with the front side. The dimensions of the building are 13.6 m × 12.4 m, with an elevation of 3 m for each story and 308.48 m^2 of living area. The overhang was installed as the main shading system with a depth (projection) of 0.5 m. The initial angle of the pitched roof was kept as 27°. The WWR was kept at 5% and the height of the windows was 1.5 m. Table 4 represents the thermophysical properties of the building envelope materials. This building was used as a base model for the energy analysis in all of the selected cities.

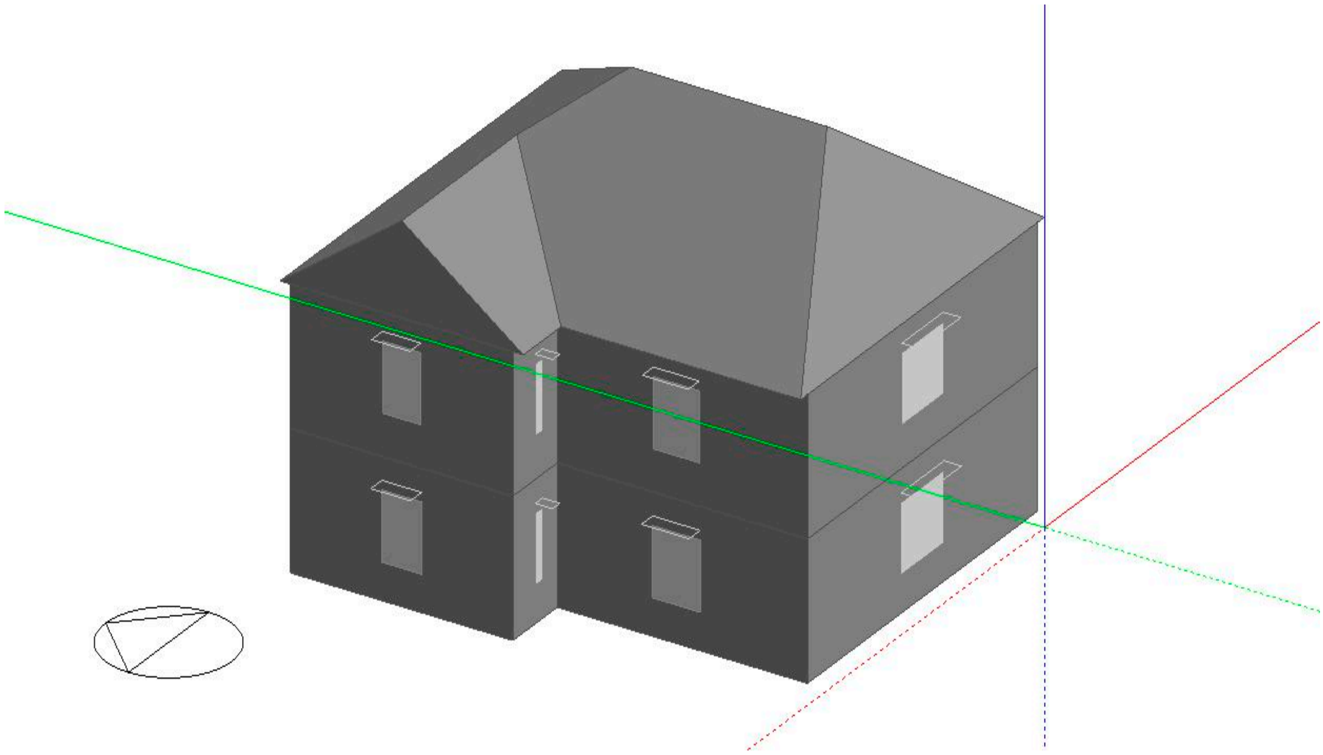

Figure 8. Model of a townhouse.

3. Results and Discussion

3.1. The Optimum Heating and Cooling Loads Reduction for Entire the Year

In this section, the numerical model for energy estimation reduced the heating and cooling loads by optimizing the building envelope parameters in seven different cities of Kazakhstan: Nur-Sultan, Almaty, Karaganda, Aktobe, Atyrau, Semey, Kokshetau. For analysis, various types of wall composition materials, angle of a pitched roof, depth of the overhang shading system and WWR were analyzed, and the HVAC system was turned off. Switching off the HVAC system allowed a detailed analysis of the building properties only in terms of heat transfer due to the climate conditions. The main purpose of this section is to demonstrate the effect of the thermal performance of building envelope components on the reduction of heating and cooling energy consumption by optimizing it based on the local climatic dataset. The results of seasonal heating (13 October–12 May) and cooling (13 May–12 October) energy for all cities are estimated and summarized in Table 6. From the obtained results, it is clearly seen that the amount of heating energy dominates almost in all cities and an average reduction of heating load for all cities was counted as 6157.8 kWh (or 5.29 Gcal) and an average reduction of building energy for cooling purposes was estimated as 1912.17 kWh (or 1.64 Gcal) due to the optimization of the numerical model. Since the optimized model is based on optimized variables, a cross-section of wall composition materials for the base and optimized cases are shown in Figure 9. The average percentage values for heating and cooling energy were reduced by 16.59% and 16.53% for heating and cooling seasons, respectively.

The maximum annual reductions of heating energy were witnessed in Koksetau city (6967.89 kWh), followed by Nur-Sultan city (6943.66 kWh). The lowest results in heating reduction were witnessed in Almaty (4758.35 kWh). On contrary, this city showed the maximum reductions in cooling energy (2107.94 kWh). The minimum reductions in the cooling energy were in Aktobe (1591.77 kWh). The overall maximum reductions achieved for optimal design to base design were fairly consistent among the selected cities and ranged between 16.59% and 16.53% for heating and cooling seasons, respectively.

Table 6. The heating and cooling energy results for the base case and optimized building model.

	Heating Load (kWh)		Heating Load		Cooling Load		Cooling Load	
List of Cities	**Base Design**	**Optimized Design**	**Reduction in (kWh)**	**Reduction (Gcal)**	**Base Design**	**Optimized Design**	**Reduction in (kWh)**	**Reduction (Gcal)**
Nur-Sultan	41,848.71	34,905.05	6943.66	5.9701	11,538.66	9614.50	1924.16	1.6543
Almaty	28,673.86	23,915.51	4758.35	4.0912	13,453.56	11,345.62	2107.94	1.8124
Karaganda	40,564.44	33,833.53	6730.91	5.7872	12,280.95	10,233.19	2047.76	1.7606
Aktobe	38,536.64	32,142.22	6394.42	5.4979	9546.91	7955.13	1591.77	1.3686
Atyrau	30,500.17	25,439.52	5060.65	4.3511	12,213.90	10,179.55	2034.35	1.7491
Semey	37,651.78	31,402.88	6248.90	5.3728	10,304.82	8586.62	1718.19	1.4773
Kokshetau	41,996.78	35,028.89	6967.89	5.9909	11,759.43	9798.42	1961.01	1.6860
Average:	37,110.34	30,952.51	6157.82	5.2983	11,585.46	9673.29	1912.17	1.6453

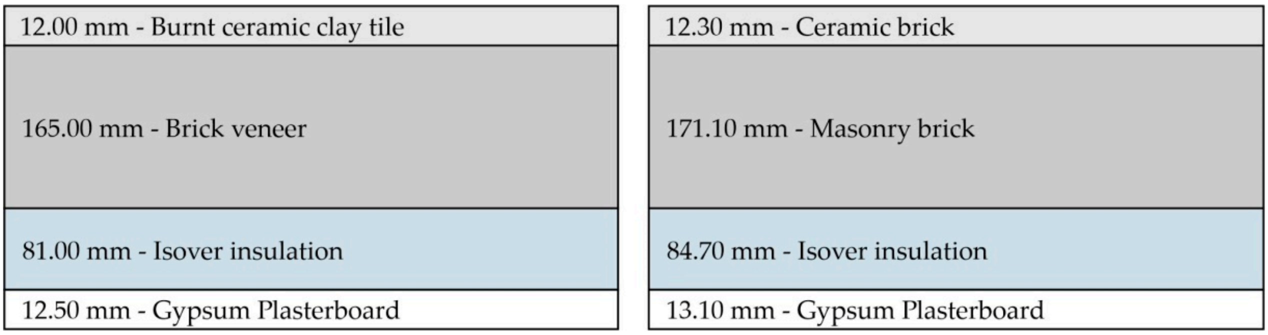

(**a**) (**b**)

Figure 9. Wall composition materials for (**a**) base case and (**b**) optimized building model.

The monthly results (Table 7) are summarized to identify the energy consumption (in kWh) of the building for each city. It can be observed from Table 7, that in January, Nur-Sultan and Kokshetau cities showed the largest amount of energy consumption in kWh. Although, in July, Atyrau and Almaty showed the highest performance in cooling energy demand. In May, as a month when the heating season ends and the cooling season starts, the average energy consumption of around 1000 kWh was obtained for the base and 900 kWh for the optimized building envelope case in each selected city. In the same way, the energy consumption for heating/cooling purposes in September shows the lowest energy performance in each city, approximately 500 kWh, representing the ending of the cooling season and starting of the heating season. In general, Table 7 demonstrated, that heating energy dominates in all analyzed cities of Kazakhstan, as energy consumption in January, February and December are the highest in each city. Thus, total energy consumption in all months for heating and cooling proves that the climatic zone of Kazakhstan is mostly heating-predominant.

The energy consumption reduction values in Kazakhstan cities can be considered as significant, especially for the construction stage of a building calculated per unit living area. The average energy consumption value for the base and optimized envelope models were 120 kWh/m^2 and 100 kWh/m^2, respectively, during the hot season. For the cool season, selected Kazakhstan's cities demonstrated an average value of 38 kWh/m^2 and 30 kWh/m^2 for the base and optimized building models, respectively. Several literature values are pertinent for this research concerning the existing Kazakhstani buildings and thermal demand. The average heating energy consumption for residential buildings in Switzerland was reported to be 101 kWh/m^2 in 2018 [48]. According to [49], the annual energy use performances across three Canadian cities, such as Quebec, Toronto, and Vancouver, are 126.08 kWh/m^2, 116.47 kWh/m^2, and 98.47 kWh/m^2 for the period from 1998 to 2014, respectively, and 126.03 kWh/m^2, 115.31 kWh/m^2, and 100.25 kWh/m^2, respectively, according to forecasting future climate conditions.

An orientation-related change can affect the optimized amount of the energy load of the building [50]. The building orientation affects the heat gains of the building, thus the diversity of solar radiation at different angles [50]. It is obviously observed, that on the current analyzed stage, the most valuable portion of the heat gain or loss mechanism of the building is carried out by solar exposure. The details of the HVAC system, namely as an effect of lightning, occupancy, hot water usage, and electronic devices, were not definitely influenced in this analysis, and the energy consumption results were based on climate impacted power usage to cool or heat the indoor area. The optimized energy consumption data for each orientation (west, north, east, and south) were obtained and the results are presented in Table 8. According to the table, when the models were directed to the south, the optimized buildings showed the highest reduction in energy consumption. On the other hand, in the cooling load-dominated season, the building directed towards the north side showed better performance for the optimized value of energy consumption. To be exact, directing the front side of the building towards the south in the cold season and north in the hot season demonstrated approximately 21% and 32% reductions, respectively, based on solar entrance into the building.

From the sun path diagram shown in Figure 10, it is seen that the north wall was less exposed to solar light within the daytime. Thus, for a better energy-saving performance in the cold season, the wall with the highest number of windows should be directed in the south direction. Alshboul and Alkurdi [51] discovered that orienting the largest glass area to the south allowed the building to gain the required heat in winter. In contrast, for the hot season, it was better to locate most of the living areas directed to the north side in a shaded direction. Finally, the suggested primary optimal design solution included suggested building orientation to the south, a combination of 0.7 m of the depth of the overhang shading system and a WWR of 4%, 12.30 mm ceramic brick as the exterior finish, 171.10 mm masonry brick as the core layer, 84.7 mm glasswool, and 13.10 mm plasterboard as the interior finish (Figure 9b).

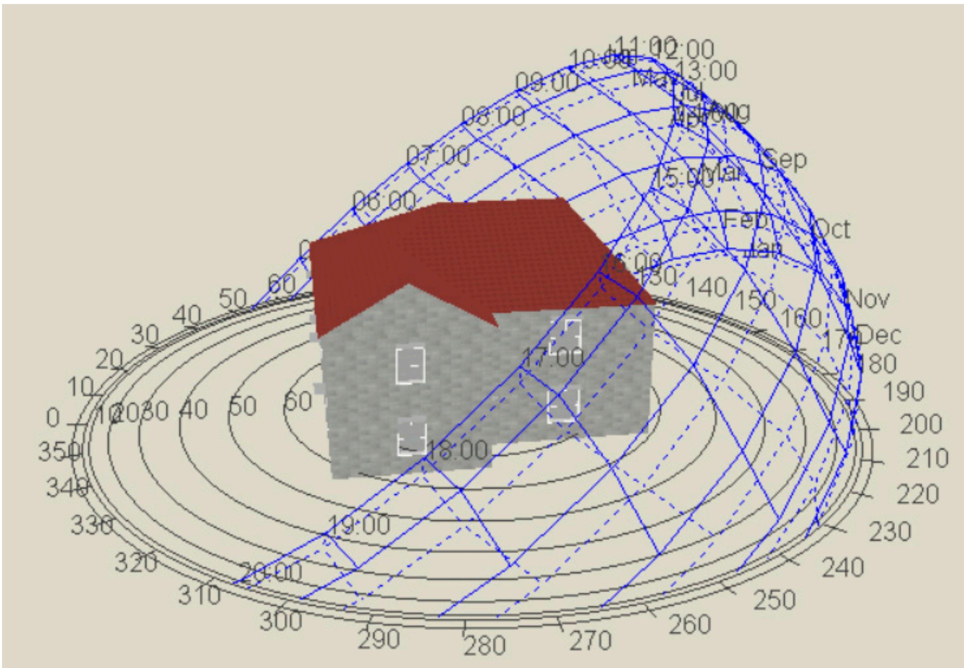

Figure 10. Sun path diagram.

Table 7. Monthly results of energy consumption for each city (kWh).

	Nur-Sultan		Almaty		Aktobe		Atyrau		Karaganda		Semey		Kokshetau	
Months	**Base**	**Optimized**	**Base**	**Optimized**	**Base**	**Optimized**	**Base**	**Optimized**	**Base**	**Optimized**	**Base**	**Optimized**	**Base**	**Optimized**
January	10,009	8349	6858	5720	9217	7688	7295	6085	9702	8092	9006	7511	10,045	8378
February	7436	6202	5095	4249	6847	5711	5419	4520	7207	6011	6690	5580	7462	6224
March	4671	3896	3200	2669	4301	3588	3404	2839	4528	3776	4203	3505	4688	3910
April	3050	2544	2090	1743	2809	2343	2223	1854	2957	2466	2745	2289	3061	2553
May	1239	1034	849	708	1141	952	903	753	1201	1002	1115	930	1244	1037
June	1846	1538	1119	932	1528	1273	1954	1629	1965	1637	1649	1374	1882	1568
July	4846	4038	2936	2447	4010	3341	5130	4275	5158	4298	4328	3606	4939	4115
August	4269	3557	2587	2156	3532	2943	4519	3766	4544	3786	3813	3177	4351	3625
September	577	481	350	291	477	398	611	509	614	512	515	429	588	490
October	2574	2147	1764	1471	2370	1977	1876	1565	2495	2081	2316	1931	2583	2154
November	4957	4135	3396	2833	4565	3807	3613	3013	4805	4008	4460	3720	4975	4149
December	7912	6599	5421	4522	7286	6077	5767	4810	7669	6397	7119	5937	7940	6623

Table 8. Optimized heating energy results of building oriented based on the front site direction.

List of Cities	**Heating (kWh)**					**Cooling (kWh)**				
	Base Design	**Optimized Design**				**Base Design**	**Optimized Design**			
		West	**North**	**East**	**South**		**West**	**North**	**East**	**South**
Nur-Sultan	41,848.71	34,905.05	33,405.05	36,405.05	33,205.05	11,538.66	9614.50	7914.50	11,114.50	8114.50
Almaty	28,673.86	23,915.51	22,415.51	25,415.51	22,215.51	13,453.56	5825.71	4125.71	7325.71	4325.71
Aktobe	38,536.64	32,142.22	30,642.22	33,642.22	30,442.22	9546.91	7955.13	6255.13	9455.13	6455.13
Karaganda	40,564.44	33,833.53	32,333.53	35,333.53	32,133.53	12,280.95	10,233.19	8533.19	11,733.19	8733.19
Atyrau	30,500.17	25,439.52	23,939.52	26,939.52	23,739.52	12,213.90	10,179.55	8479.55	11,679.55	8679.55
Kokshetau	41,996.78	35,028.89	33,528.89	36,528.89	33,328.89	11,759.43	9798.42	8098.42	11,298.42	8298.42
Semey	37,651.78	31,402.88	29,902.88	32,902.88	29,702.88	10,304.82	8586.62	6886.62	10,086.62	7086.62

The contribution of each building envelope component for the heat transfer was calculated in percentage rates, to simply point out the further investigation of the optimization goals for energy reduction. As Nur-Sultan and Kokshetau showed the highest results for the heating energy consumption, the energy consumption reduction by building envelope components are shown in Table 9, where 16.592% was the total heating energy reduction in Nur-Sultan city, while 6.37%, 1.61%, 8.64%, and 0.3% contribution rates of this reduction corresponded to the wall, window glazing, roofing, and shading systems, respectively. For Kokshetau, the contribution rate was almost identical to Nur-Sultan. For a cooling period, Almaty and Atyrau were selected for this analysis with the highest cooling energy reduction, showing 16.668% and 16.656%, respectively, corresponding to the base case performance. In Almaty, the contribution for cooling energy reduction was 5.88% from an opaque wall, 1.48% from window glazing, 8.14% from roofing, and around 1.2% from the shading system, while for Atyrau, the contribution for reduction was around 6.42% from the opaque wall, 1.62% from the window glazing, 8.36% from the roofing, and around 0.75% from the shading system (Table 9). This result indicates that the wall and the roof had a considerable impact on energy consumption in all of the analyzed cities. The energy reduction value for window glazing was similar in all cities. Shading systems could reduce energy consumption in cities located in the south and west parts of the country, while its impact was negligible in the cities located in the north part.

Overall, the results obtained in this research verified the effectiveness of the proposed BESM and optimization in enhancing the energy efficiency of the residential buildings. In addition, the results showed that the design variables and orientation were important and had a noteworthy impact on building energy efficiency, therefore energy consumption may be significantly reduced by selecting appropriate building orientation and wall composition materials.

Table 9. Energy reduction by building envelope components during the hot and cold seasons in Nur-Sultan, Kokshetau, Almaty, and Atyrau.

Envelope Components	Heating Energy Reduction (kWh) in Nur-Sultan			Heating Energy Reduction (kWh) in Koksetau		
	Base Case	Optimized Case	Percentage of Contribution for Energy Reduction	Base Case	Optimized Case	Percentage of Contribution for Energy Reduction
Wall	16,095.01	13,410.52	6.37	16,156.16	13,461.60	6.38
Window	4067.69	3385.79	1.61	4069.49	3397.80	1.61
Roof	22,309.55	18,590.43	8.84	22,384.28	18,652.88	8.83
Shading system	523.11	624.80	0.30	524.96	630.52	0.30
Total	41,848.71	34,905.05	16.592	41,996.78	35,028.89	16.591
	Cooling Energy Reduction (kWh) in Almaty			Cooling Energy Reduction (kWh) in Atyrau		
Wall	4802.92	4005.00	5.88	4702.35	3922.18	6.42
Window	1210.82	1008.63	1.48	1184.75	987.42	1.62
Roof	6713.33	5544.61	8.15	6143.59	5124.38	8.38
Shading system	980.76	816.88	1.20	549.63	458.08	0.75
Total	13,454	11,346	16.668	12,214	10,180	16.656

3.2. Economic Benefit of the Optimization

An economic assessment was conducted on the optimized buildings considering energy savings and economic benefits. According to the Ministry of Energy of the Republic of Kazakhstan, the average 3000 tenges (₸) per Gcal. Meanwhile, money spent on heating energy for residents of the Kokshetau was established as 1600 tenges per Gcal. In other regions, this tariff costs over 2000 tenges. The highest tariffs were observed in Almaty and

Atyrau, such as over 4000 tenges per Gcal. The average cost of electricity supply for the population reached 12.69 tenges per kWh. The lowest rates of electricity tariff are marked in the west and north regions of the country. At the same time, in the Atyrau region, the cost per kWh did not even reach 5 tenges. On contrary, this figure rate is 17.12 tenge per kWh in Almaty. The current electricity tariffs for the selected cities separately for central heating and electricity-based equipment for heating and cooling are shown in Table 10 [49].

Table 10. Economic analysis for the heating and cooling energy savings for the optimized building configuration.

List of Cities	Energy Reduction (kWh)	Energy Reduction (Gcal)	Price Rate (₸ per Gcal)	Price Rate (₸ per kWh)	Economic Impact (₸ for the Period)	
					Centralized Heating	Equipment Heating
Heating Energy Reduction						
Nur-Sultan	6943.66	5.97	2176.76	11.93	12,996	82,838
Almaty	4758.35	4.09	4881.79	17.12	19,973	81,463
Karaganda	6394.42	5.49	2758.57	8.75	15,166	55,951
Aktobe	6730.91	5.79	3042.32	10.02	17,607	67,444
Atyrau	5060.65	4.35	4832.88	4.73	21,029	23,937
Semey	6967.89	5.99	1611.98	17.11	9657	119,221
Kokshetau	6248.90	5.37	3018.12	10.395	16,216	64,957
Cooling Energy Reduction						
Nur-Sultan	1924.16	1.65	11.93		22,955	
Almaty	2107.94	1.81	17.12		36,088	
Karaganda	2047.77	1.76	10.02		20,519	
Aktobe	1591.77	1.36	8.75		13,928	
Atyrau	2034.35	1.74	4.73		9622	
Semey	1718.19	1.47	10.395		17,861	
Kokshetau	1961.00	1.68	17.11		33,553	

On the contrary, Atyrau and Kokshetau showed the lowest cost reduction for equipment-based heating and centralized heating, with 24,000 ₸ and 9700 ₸, respectively. Regarding the payment reduction for air-conditioning during the cooling season (from 13 May to 12 October), Almaty and Atyrau showed the highest and lowest reductions, namely, 36,000 ₸ and 9600 ₸, respectively. Compared with the base case, the optimal design in the envelope entails the energy efficiency for heating and cooling with a significant reduction in energy service charges. Thus, the energy demand can be affected by the heat gain and heat loss through building envelope during hot and cold seasons. In other words, the shading systems characteristics, wall and roof properties, and window-to-wall ratio were optimized using a single-objective optimization to reduce the fees charged for heating and cooling energy.

4. Conclusions

In this research, the energy performance of the townhouse for cold and hot seasons by optimizing the envelope characteristics in seven cities of Kazakhstan for energy consumption and cost reduction was investigated. To conduct the analysis, the selected cities were as follows: Nur-Sultan, Almaty, Karaganda, Aktobe, Atyrau, Kokshetau, and Semey. The OTTV-based numerical model was developed for the estimation of the energy transfer mechanism through the envelope components of the base case. The brute force algorithm was used to optimize the numerical model for reducing the value of energy performance in cold and hot seasons by searching the optimum variant of wall components, the thickness of the wall, WWR, depth of the shading system, and angle of the pitched roof. The energy reduction for hot (13 October–12 May) and cold (13 May–12 October) seasons were conducted by using brute force algorithm optimization with Python coding software. The OTTV-based numerical model was developed and implemented in exhaustive search optimization for energy-saving purposes by searching for the optimum envelope configurations. The main conclusions and recommendations are summarized below:

- This research has shown that proper selection of design variables can lead to notable energy savings in all cities. Due to the optimization of the numerical model analyzing the heat transfer through the envelope, the average annual heating reduction was 6156.8 kWh (or 5.29 Gcal), and the average cooling energy reduction was 1912.17 kWh (or 1.64 Gcal). In terms of percentage, heating and cooling energy were reduced by 16.59% and 16.69%, respectively. It is also concluded that the heating energy savings effect was more evident in the cities located in the northern part of Kazakstan (Nur-Sultan and Kokshetau), and the effect of the cooling energy savings was evident in the southern part (Almaty);
- Regarding monthly energy consumption, January, February, and December showed the highest energy consumption in each city. Overall energy consumption for heating and cooling throughout all months demonstrated that Kazakhstan's climatic zone is mostly heating-dominated;
- The results showed that proper selection of orientation is critical. The direction of the frontage of the building towards the south in the cold season and north in the hot season showed around 21% and 32% energy reduction, respectively, which were effective compared with an initial orientation of the building;
- The building orientation to the south, a combination of 0.7 m of the depth of the overhang shading system and the WWR of 4%, 12.30 mm ceramic brick as exterior finish, 171.10 mm masonry brick as core layer, 84.7 mm glasswool, and 13.10 mm plasterboard as the interior finish was found to be optimal design solution;
- From the economic analysis, it was found that equipment heating had a high-cost reduction compared to central heating. The highest cost reduction was observed in Atyrau with central heating and in Kokshetau with equipment-based heating, for cooling in Almaty. This highlights the fact that optimization of buildings brings significant economic benefits.

From the operational view point, it is suggested that for future work, the proposed analysis should take into account occupancy rate and the working schedule of HVAC considering the opening rate of external doors and windows. It is suggested that the numerical analysis should be done to increase the optimisation variables, e.g., roof composition materials and detailed properties of the windows in terms of the type and material configurations. The space total energy demand for heating and cooling for residential buildings in Kazakhstan cities is crucial to be investigated, as zero-energy buildings should be designed due to the forecast of shortage of electrical energy.

Author Contributions: Conceptualization, M.K. and S.A.M.; methodology, M.K. and S.A.M.; software, M.K.; validation, M.K. and S.A.M.; formal analysis, M.K.; investigation, M.K. and S.A.M.; resources, M.K.; data curation, M.K. and S.A.M.; writing—original draft preparation, M.K.; writing—review and editing, M.K., S.A.M. and A.S.; visualization, M.K. and S.A.M.; supervision, S.A.M.; project administration, S.A.M.; funding acquisition, S.A.M. and J.R.K. All authors have read and agreed to the published version of the manuscript.

Funding: This research was supported by Nazarbayev University Faculty development competitive research grants number 021220FD0651 and SOE2017004.

Institutional Review Board Statement: Not applicable.

Informed Consent Statement: Not applicable.

Data Availability Statement: The data presented in this research are available upon request from the corresponding author.

Conflicts of Interest: The authors declare no conflict of interest.

Abbreviations

TDES	Total direct energy supply
TFEC	Total final energy consumption
PLA	Perimeter Annual Load
ENVLOAD	Envelope Energy Load
OTTV	Overall Thermal Transfer Value
TRNSYS	Transient System Simulation Tool
GMDH	Grouped Method of Data Handling type neural network
NSGA-II	Non-Dominated Sorting Genetic Algorithm II
ASHRAE	The American Society of Heating, Refrigerating and Air-Conditioning Engineers
HVAC	Heating, ventilation, and air conditioning
PCM	Phase change material
WNN	Wavelet neural network
MLP	Multi-Layer Perceptron neural network
ACO	Ant Colony Optimization
ABC	Artificial Bee Colony
PSO	Particle Swarm Optimization
BF	Brute force
BESM	Building Energy Simulation model
ETTV	Envelope Thermal Transfer Value
RTTV	Roof Transfer Value
SHGC	Standard solar heat gain coefficient of glazing
WWR	Window-to-wall ratio
A_w, A_g, A_r	Surface area of the wall, fenestration, and roof
k_w	An overall thermal conductivity of the wall
k_r	Thermal conductivity values of the roof
U_g	U-value of glazing
A_{wall}	The exterior wall's gross area
A_{wsi}	Wall area exposed to solar radiation
Q_c	Heat gain through the envelope for the cooling season
Q_h	Heat loss through the envelope for the heating season
Q_{gsol}	Solar radiation through the fenestration
h_1, h_2, h_3, h_4	Thicknesses of wall composition layers
C_1, C_2, C_3, C_4	Thermal conductivity values of wall composition layers
R_c	Thermal resistance value for roof ceiling
R_r	Thermal resistance value for the roof
A_c	Ceiling area
A_r	Roof area
A_T	Total area building's wall
SLF	Shade line factor
D_{oh}	The depth of overhang (projection)
X_{oh}	Vertical offset from the top of the window to overhang
h_g	The height of the window
SC_g	Shading coefficient of the glazing
SC	Total shading coefficient
α	The solar absorptivity constant related to the façade surface and color
TD	Equivalent temperature difference
TD_w, TD_r, TD_g	Equivalent temperature differences between indoor and outdoor surrounding space wall, roof, and glazing
ESM	External shading multiplier
SF	Solar factor
q	The standard solar heat gain factor

References

1. Wang, X.; Zheng, H.; Wang, Z.; Shan, Y.; Meng, J.; Liang, X.; Feng, K.; Guan, D. Kazakhstan's CO_2 emissions in the post-Kyoto Protocol era: Production- and consumption-based analysis. *J. Environ. Manag.* **2019**, *249*, 109393. [CrossRef] [PubMed]
2. Sarbassov, Y.; Kerimray, A.; Tokmurzin, D.; Tosato, G.; De Miglio, R. Electricity and heating system in Kazakhstan: Exploring energy efficiency improvement paths. *Energy Policy* **2013**, *60*, 431–444. [CrossRef]

3. Assenova, B. What Is the Housing Stock in Kazakhstan—NewTimes.kz 2019. Available online: https://newtimes.kz/obshchestvo/96182-chto-iz-sebya-predstavlyaet-zhilishchnyj-fond-v-kazakhstane (accessed on 23 November 2021).
4. History of Housing Construction in Kazakhstan. 2020. Available online: https://google-info.org/7523418/1/istoriya-zhilishchnogo-stroitelstva-v-kazakhstane.html (accessed on 24 November 2021).
5. Agency for Strategic Planning and Reforms of the Republic of Kazakhstan Bureau of National Statistics n.d. Available online: https://stat.gov.kz/search (accessed on 24 November 2021).
6. Energy-Efficient Design and Construction of Residential Buildings. United Nations, Development Programme, PIMS No. 4133 Atlas Award 00059795, Project ID 0074950. Available online: https://www.kz.undp.org/content/kazakhstan/en/home/operations/projects/environment_and_energy/energy-efficient-design-and-construction-of-residential-building.html (accessed on 27 November 2021).
7. Imani, N.; Vale, B. A framework for finding inspiration in nature: Biomimetic energy efficient building design. *Energy Build.* **2020**, *225*, 110296. [CrossRef]
8. Yu, J.; Yang, C.; Tian, L.; Liao, D. Evaluation on energy and thermal performance for residential envelopes in hot summer and cold winter zone of China. *Appl. Energy* **2009**, *86*, 1970–1985. [CrossRef]
9. Huang, J.; Deringer, J. *Status of Energy Efficient Building Codes in Asia*; The Asia Business Council: Hong Kong, China, 2017; pp. 6–9.
10. Lin, Y.-H.; Tsai, K.-T.; Lin, M.-D.; Yang, M.-D. Design optimization of office building envelope configurations for energy conservation. *Appl. Energy* **2016**, *171*, 336–346. [CrossRef]
11. Yang, K.; Hwang, R.-L. Energy conservation of buildings in Taiwan. *Pattern Recognit.* **1995**, *28*, 1483–1491. [CrossRef]
12. Yang, K.H.; Hwang, R.L. The analysis of design strategies on building energy conservation in Taiwan. *Build. Environ.* **1993**, *28*, 429–438. [CrossRef]
13. Yang, K.-H.; Hwang, R.-L. An improved assessment model of variable frequency-driven direct expansion air-conditioning system in commercial buildings for Taiwan green building rating system. *Build. Environ.* **2007**, *42*, 3582–3588. [CrossRef]
14. Huang, K.T.; Lin, H.T. Design standard of energy conservation for building hvac system—A simplified method of chiller capacity estimation based on building envelope energy conservation index in taiwan. In Proceedings of the IBPSA 2005—International Building Performance Simulation Association 2005, Montréal, QC, Canada, 15–18 August 2005; pp. 435–442.
15. Chan, A.; Chow, T. Calculation of overall thermal transfer value (OTTV) for commercial buildings constructed with naturally ventilated double skin façade in subtropical Hong Kong. *Energy Build.* **2014**, *69*, 14–21. [CrossRef]
16. Guo, J.; Hermelin, D.; Komusiewicz, C. Local search for string problems: Brute-force is essentially optimal. *Theor. Comput. Sci.* **2014**, *525*, 30–41. [CrossRef]
17. Robinson, A.C.; Quinn, S.D. A brute force method for spatially-enhanced multivariate facet analysis. *Comput. Environ. Urban Syst.* **2018**, *69*, 28–38. [CrossRef]
18. Al-Saadi, S.N.J.; Al-Jabri, K.S. Energy-efficient envelope design for residential buildings: A case study in Oman. In Proceedings of the 2017 Smart Cities Symp Prague, SCSP 2017—IEEE Proceedings 2017, Prague, Czech Republic, 25–26 May 2017. [CrossRef]
19. Hui Sam, C.M. Overall thermal transfer value (OTTV): How to improve its control in Hong Kong. In Proceedings of the One-day Symposium on Building, Energy and Environment, Hong Kong, China, 16 October 1997; Volume 16, pp. 12-1–12-11.
20. Devgan, S.; Jain, A.; Bhattacharjee, B. Predetermined overall thermal transfer value coefficients for Composite, Hot-Dry and Warm-Humid climates. *Energy Build.* **2010**, *42*, 1841–1861. [CrossRef]
21. Chan, L.S. Investigating the thermal performance and Overall Thermal Transfer Value (OTTV) of air-conditioned buildings under the effect of adjacent shading against solar radiation. *J. Build. Eng.* **2021**, *44*, 103211. [CrossRef]
22. Chou, S.K.; Chang, W.L. Development of an energy-estimating equation for large commercial buildings. *Int. J. Energy Res.* **1993**, *17*, 759–773. [CrossRef]
23. Djamila, H.; Rajin, M.; Rizalman, A.N. Energy efficiency through building envelope in Malaysia and Singapore. *J. Adv. Res. Fluid Mech. Therm. Sci.* **2018**, *46*, 96–105.
24. Zhang, Y.; Long, E.; Li, Y.; Li, P. Solar radiation reflective coating material on building envelopes: Heat transfer analysis and cooling energy saving. *Energy Explor. Exploit.* **2017**, *35*, 748–766. [CrossRef]
25. Mustafaraj, G.; Marini, D.; Costa, A.; Keane, M. Model calibration for building energy efficiency simulation. *Appl. Energy* **2014**, *130*, 72–85. [CrossRef]
26. Kutlu, L.; Tran, K.C.; Tsionas, M.G. A spatial stochastic frontier model with endogenous frontier and environmental variables. *Eur. J. Oper. Res.* **2020**, *286*, 389–399. [CrossRef]
27. Lleras, C. Path Analysis. *Encycl. Soc. Meas.* **2005**, *3*, 25–30. [CrossRef]
28. Zhang, Y.; Sun, X.; Medina, M.A. Calculation of transient phase change heat transfer through building envelopes: An improved enthalpy model and error analysis. *Energy Build.* **2020**, *209*, 109673. [CrossRef]
29. White Box Technologies Weather Data, n.d. Available online: http://weather.whiteboxtechnologies.com/ (accessed on 24 November 2021).
30. Xing, F.; Mohotti, D.; Chauhan, K. Study on localised wind pressure development in gable roof buildings having different roof pitches with experiments, RANS and LES simulation models. *Build. Environ.* **2018**, *143*, 240–257. [CrossRef]
31. Çengel, Y.; Ghajar, R.A. Heat and Mass Transfer: Fundamentals & Applications. 2015. Available online: https://studylib.net/doc/8394668/heating-and-cooling-of-buildings (accessed on 8 December 2021).

32. Shen, H.; Tzempelikos, A. Daylighting and energy analysis of private offices with automated interior roller shades. *Sol. Energy* **2012**, *86*, 681–704. [CrossRef]
33. Barnaby, C.S.; Wright, J.L.; Collins, M.R. Improving load calculations for fenestration with shading devices. *ASHRAE Trans.* **2009**, *115*, 31–44.
34. Kotey, N.A.; Wright, J.L.; Barnaby, C.S.; Collins, M.R. Solar gain through windows with shading devices: Simulation versus measurement. *ASHRAE Trans.* **2009**, *115*, 18–30.
35. Bessoudo, M.; Tzempelikos, A.; Athienitis, A.; Zmeureanu, R. Indoor thermal environmental conditions near glazed facades with shading devices—Part I: Experiments and building thermal model. *Build. Environ.* **2010**, *45*, 2506–2516. [CrossRef]
36. DesignBuilder Software Ltd.—Previous Versions n.d. Available online: https://designbuilder.co.uk/download/previous-versions (accessed on 22 October 2021).
37. Residential Cooling and Heating Load Calculations. In *ASHRAE Handbook of Fundamentals*; SI Edition; ASHRAE: Atlanta, GA, USA, 2017; Chapter 17.
38. Ozmen, Y.; Baydar, E.; van Beeck, J. Wind flow over the low-rise building models with gabled roofs having different pitch angles. *Build. Environ.* **2016**, *95*, 63–74. [CrossRef]
39. Szcześniak, J.T.; Ang, Y.Q.; Letellier-Duchesne, S.; Reinhart, C.F. A method for using street view imagery to auto-extract window-to-wall ratios and its relevance for urban-level daylighting and energy simulations. *Build. Environ.* **2021**, *2021*, 108108. [CrossRef]
40. Xue, P.; Li, Q.; Xie, J.; Zhao, M.; Liu, J. Optimization of window-to-wall ratio with sunshades in China low latitude region considering daylighting and energy saving requirements. *Appl. Energy* **2019**, *233–234*, 62–70. [CrossRef]
41. GOST 530-2012. Interstate Standard. Ceramic Brick and Stone. General Specifications. 2012. Available online: https://docs.cntd.ru/document/1200100260 (accessed on 27 November 2021).
42. GOST 9573-2012. Interstate Standard. Thermal Insulating Plates of Mineral Wool on Syntetic Binder. Specifications. 2013, pp. 14–27. Available online: https://docs.cntd.ru/document/1200101613 (accessed on 27 November 2021).
43. SN RK 2.04-04-2011. State Standards in the Field of Architecture, Urban Planning and Construction. Thermal Protection of Buildings. 2011. Available online: http://www.hoffmann.kz/files/12_SN_RK_2-04-04-2011.pdf (accessed on 27 November 2021).
44. GOST 24992-81. State Standard of the Union of SSR. Masonary Structures. Method of Estimating Bonding Strength in Masonry. 1995. Available online: http://gostrf.com/normadata/1/4294853/4294853407.html (accessed on 27 November 2021).
45. GOST 31310-2015. Interstate Standard. Wall Three-Layer Reinforced Concrete Panels with Enerqy-Efficient Insulation. General Specifications. Interstate Council for Standardization, Metrology and Certification (isc). 2017. Available online: https://docs.cntd.ru/document/1200133283 (accessed on 27 November 2021).
46. Peel, M.C.; Finlayson, B.L.; McMahon, T.A. Updated world map of the Köppen-Geiger climate classification. *Hydrol. Earth Syst. Sci.* **2007**, *11*, 1633–1644. [CrossRef]
47. Climate Data for Cities Worldwide—Climate-Data.org n.d. Available online: https://en.climate-data.org/ (accessed on 22 October 2021).
48. Mutschler, R.; Rüdisüli, M.; Heer, P.; Eggimann, S. Benchmarking cooling and heating energy demands considering climate change, population growth and cooling device uptake. *Appl. Energy* **2021**, *288*, 116636. [CrossRef]
49. Tootkaboni, M.P.; Ballarini, I.; Corrado, V. Analysing the future energy performance of residential buildings in the most populated Italian climatic zone: A study of climate change impacts. *Energy Rep.* **2021**, *7*, 8548–8560. [CrossRef]
50. Albatayneh, A. Optimising the Parameters of a Building Envelope in the East Mediterranean Saharan, Cool Climate Zone. *Buildings* **2021**, *11*, 43. [CrossRef]
51. Alshboul, A.A.; Alkurdi, N.Y. Enhancing the Strategies of Climate Responsive Architecture, The Study of Solar Accessibility for Buildings Standing on Sloped Sites. *Mod. Appl. Sci.* **2018**, *13*, 69. [CrossRef]